



Published in final edited form as:

Abdom Imaging. 2015 April ; 40(4): 745–759. doi:10.1007/s00261-014-0315-6.

Magnetic Resonance Elastography of Abdomen

Sudhakar K. Venkatesh, M.D.¹ and Richard L. Ehman, M.D.¹

¹Department of Radiology, Mayo Clinic College of Medicine, Rochester, MN

Abstract

Many diseases cause substantial changes in the mechanical properties of tissue and this provides motivation for developing methods to non-invasively assess the stiffness of tissue using imaging technology. Magnetic resonance elastography (MRE) has emerged as a versatile MRI-based technique, based on direct visualization of propagating shear waves in the tissues. The most established clinical application of MRE in the abdomen is in chronic liver disease. MRE is currently regarded as the most accurate non-invasive technique for detection and staging of liver fibrosis. Increasing experience and ongoing research is leading to exploration of applications in other abdominal organs. In this review article, the current use of MRE in liver disease and the potential future applications of this technology in other parts of the abdomen are surveyed.

Keywords

Magnetic resonance elastography; liver; spleen; kidney; pancreas; uterus; liver fibrosis

Elastography

Mechanical properties of pathological tissues are often markedly different from those of normal tissues. With palpation, clinicians can evaluate the “stiffness” of tissues and this technique is often used to detect tumors in accessible regions of the body such as the breast, thyroid, and prostate. Deeper structures, however, such as liver, spleen and kidneys are much less accessible to palpation. Recognizing the potential diagnostic value of quantitatively evaluating the mechanical properties of tissue, several imaging-based “elastography” methods have been developed. The stiffness of human tissues (normal and abnormal) is spread over a wider range (several orders of magnitude) in contrast to other physical properties like x-ray attenuation coefficient, T1-relaxation or bulk modulus (fig.1). The most commonly available quantitative elastography techniques currently used in clinical radiology are ultrasound-based shear wave elastography and MRI-based magnetic resonance elastography (MRE).

These dynamic elastography techniques exploit the fact that the propagation characteristics (such as speed) of shear waves depend on the mechanical properties of the medium. In dynamic shear wave elastography, shear waves are generated in tissue and the resulting

Address correspondence to: Sudhakar Kundapur Venkatesh, MD, vekatesh.sudhakar@mayo.edu, 200 1st St SW, Rochester, MN 55905, USA.
Mayo Clinic College of Medicine, Rochester, MN Address: 200 First St. SW, Rochester, MN 55905

Technical Approach for MRE

The basic approach for MRE consists of three steps (fig.2): 1. Generating shear waves in tissue, 2. Visualizing the propagating waves using a phase contrast sequence (MRE sequence), and 3. Processing the wave images to produce quantitative cross-sectional images depicting tissue stiffness.

Mechanical vibrations are applied to the abdomen at typical frequencies in the range of 40-200 Hz. A number of devices for generating shear waves have been described, including pneumatic, electromechanical, and piezoelectric systems [25, 37-39]. For brevity, this review focuses on the standardized pneumatic driver system that is used in current FDA-approved commercial implementations of MRE. This system uses an acoustic wave generator that is placed outside the scanner room. A disc-shaped, non-metallic drum-like “passive driver” is applied against the body wall and activated with acoustic pressure waves conducted via a 25-foot long flexible plastic tube connected to the wave generator to deliver shear waves to the tissues. The passive driver can be easily applied against the body (fig.3) and placed under surface coil arrays commonly used for abdominal imaging. Newer flexible passive driver designs have improved ergonomics and may be useful for kidney and pancreas imaging [40, 41].

The MRE acquisition is a modified phase contrast sequence [14, 42]. MRE sequences can be based on gradient recalled echo (GRE), spin echo (SE), balanced steady state free precession (SSFP), or echo planar imaging (EPI) techniques. Special motion encoding gradients (MEGs) are used to sensitize the sequence to cyclic tissue motion caused by the shear waves. These gradients oscillate at the same frequency as the acoustic vibration that allows capturing the cyclic motion caused by shear waves with amplitudes as small as fractions of microns [42-44]. The timing relationship between the applied mechanical waves and the MEG's is varied to allow snapshots of the waves in the tissue to be acquired at typically 3 or 4 phases of the wave cycle. Immediately after the wave images are acquired, the MRI system typically processes them to calculate corresponding elastograms. The wave images undergo several preprocessing steps including phase unwrapping, directional filtering and removal of gradient field effects before inversion [3]. In research studies, many different kinds of processing algorithms have been evaluated including local spatial frequency, phase gradient, direct inversion of the wave equation, and finite element-based iterative methods [3, 45-48].

The stiffness maps depict tissue stiffness across the cross-section studied. Regions of interest (ROI) can be drawn manually or using an automated segmentation algorithm to obtain shear stiffness of the organs.

MRE of Liver

The most common clinical application of MRE in the abdomen is in the evaluation of chronic liver diseases. Multiple studies have demonstrated that MRE surpasses other non-invasive tests such as serum tests for liver function [23, 24, 27] and TE [49] for detection and staging of liver fibrosis. Liver stiffness measured with MRE is not affected by the presence of liver fat alone [25]. MRE is easily performed in patients of different sizes [25,

50, 51]. MRE has high repeatability, reproducibility and interobserver correlation for liver stiffness [22, 33, 34, 52].

Most clinical studies on MRE of the liver are performed after 4-6 hours of fasting similar to a clinical liver MRI study. Follow up studies would ideally be performed with similar conditions to ensure comparability as post prandial status is known to cause increased liver stiffness in patients with liver fibrosis [53, 54]. Fasting is the best way to ensure repeatability of the liver stiffness measurements. The MRE sequence can be performed in any order during a MRI study and administration of intravenous gadolinium contrast agents do not significantly influence the stiffness evaluation [55, 56]

The most widely used MRE technique is described here (fig.4). The pneumatic passive driver is placed in the right lower chest /upper abdomen in the mid clavicular line at the level of the xiphisternum so that the largest portion of the liver is directly under the driver [51]. The 2D-GRE MRE sequence is performed at 60Hz and 4 slices of 10mm thickness is prescribed over the region of liver with the largest cross-section. This is usually near the dome of the liver but the dome should be avoided as there may be breath hold artifacts. The slices are obtained in expiration to ensure reproducibility of the position of the liver. Typical sequence parameters are as follows: repetition time/echo time (TR/TE) = 50/18.4 to 26ms; matrix = 256 ×64; band width = 33 KHz; flip angle of 30, 4 phase offsets and NEX=1. The prescribed time to echo is dependent on the sequence installed, gradient performance and adjusting other parameters. A time to echo of 18.4ms is in the In-phase and therefore beneficial in patients with fatty livers when the signal from the liver parenchyma would be the highest possible. Reducing the time to echo below 20ms may also be useful in patients with iron overload as it would marginally increase signal from the liver. Breath hold duration is about 16-20 seconds depending on the size of the patient and field of view prescribed. Using parallel imaging with an acceleration factor of 2, each section can be acquired in as short as 12 seconds.

Stiffness maps are automatically generated within few minutes of completion of the MRE sequence (fig.5). Manufacturers have standardized the color scale of the stiffness maps and have adopted a default scale of 0 to 8 kPa for liver MRE. Liver stiffness can be quantified by drawing the ROI on the gray-scale stiffness maps taking care to avoid large vessels, liver edge, fissures, and gall bladder fossa that can be visualized on the magnitude images of the MRE sequence. Regions of wave interference that can be seen on wave images are also excluded for reliable stiffness estimation. A large geographical ROI provides an assessment of a larger volume of liver than a few small elliptical ROIs. . Larger ROIs can also be drawn using an automated segmentation algorithm [57]. The average stiffness from several slices is reported as the mean stiffness value in kilopascals (kPa). Liver stiffness with MRE is reproducible with >95% interobserver agreement [24, 34, 58] and has better agreement than that between pathologists staging liver fibrosis [59].

Normal liver stiffness is usually less than 2.5 kPa [22] and most studies have reported normal liver stiffness within a range of 1.54 to 2.87kPa [50]. The influence of age, sex, race, and ethnicity on the measured normal liver parenchyma stiffness is not clearly understood, however studies have not shown any significant association. Body mass index (BMI) as a

single parameter is also not significantly associated with liver stiffness and this is an advantage over TE which often does not give reliable results in patients with high BMI that are associated with a high failure rate [21, 25, 33, 60].

Detection and staging of liver fibrosis

MRE is the most promising non-invasive technique to replace or reduce the need for invasive liver biopsy, the current gold standard for detection and staging of liver fibrosis. Estimation of fibrosis content or burden is considered to be a better indicator of mild fibrosis than histologic staging of fibrosis [61, 62]. MRE correlates well with the fibrosis content of the liver and therefore may serve as an indicator for fibrosis burden [63]. Liver stiffness increases with increasing stage of fibrosis (fig.6).

Multiple published studies have concluded that MRE has a high diagnostic performance in detection and staging of liver fibrosis. MRE can differentiate normal livers from fibrotic livers with an accuracy of 90% using a cut off of >2.4kPa [23-25, 64]. MRE can also detect liver fibrosis when anatomical features of fibrosis and cirrhosis are absent [65]. The accuracy of MRE for detecting clinically significant fibrosis and cirrhosis are >95% and 98% respectively [23-25, 35, 36, 49, 64]. The high performance of MRE has been demonstrated in chronic liver diseases of different etiologies.

MRE has a high positive predictive value for ruling in significant fibrosis and a high negative predictive value for ruling out cirrhosis which is very useful for clinical decisions in the management of chronic liver diseases [50]. It should be noted, however, that liver stiffness may be increased with severe acute inflammation of the liver (acute hepatitis), acute flare of chronic hepatitis, portal hypertension, passive congestion due to cardiac failure and acute biliary obstruction [66]. MRE of the liver for assessment of liver fibrosis is best avoided when these conditions are known to coexist. MRE may be performed when acute inflammation has resolved.

Chronic liver diseases like viral hepatitis, autoimmune hepatitis and steatohepatitis are characterized by liver fibrosis and inflammation, and studies have shown that the presence of hepatitis activity may influence liver stiffness measured with MRE [67, 68] whereas another study did not show any such influence [24]. The effect of necroinflammation leading to overestimation of liver stiffness is most significant in livers with a mild degree of fibrosis (stage 2), leading to misclassification of fibrosis [24]. Liver stiffness should therefore be interpreted carefully when serum alanine amino transferase levels are high indicating the presence of inflammation when mild fibrosis is suspected. Rarely a liver biopsy may be needed to confirm when the clinical suspicion of fibrosis is high and MRE results are not concordant.

MRE in non-alcoholic fatty liver disease (NAFLD)

NAFLD is the most common cause of chronic liver disease in adults in the United States and is increasing in prevalence among children and adolescents [69-71]. NAFLD has a spectrum consisting of simple steatosis, steatohepatitis (NASH) with or without fibrosis, and finally progression to cirrhosis and development of complications including hepatocellular

carcinoma. Patients with NASH and those with advanced fibrosis are at particularly high risk for adverse outcomes and require more intense monitoring and therapy. As mentioned earlier, the presence of fat alone does not affect the evaluation of fibrosis in the liver. Simple steatosis in isolation does not cause any increased liver stiffness, however NASH with or without fibrosis can cause increased stiffness that is readily detectable with MRE (fig.7) [72]. MRE can differentiate steatohepatitis from normal liver with an accuracy of 93% [72], and advanced fibrosis (stage 3-4) from stage 0-2 fibrosis with an accuracy of 0.92 to 0.95 [73, 74]. MRE can therefore be useful for non-invasive diagnosis of advanced fibrosis in NAFLD. With MRE and MR fat quantification techniques, MRI can serve as a one stop technique in the evaluation of NAFLD [75].

Portal hypertension and varices

Portal hypertension due to chronic liver disease results from liver fibrosis and associated architectural distortion and changes in the vasculature. Increased liver stiffness is associated with esophageal varices and is useful to predict esophageal varices [76-78]. MRE may be more accurate than TE for prediction of varices. In one study, MRE had an accuracy of 0.86 for the presence of esophageal varices and 0.81 for varices with a high bleeding risk [78], but in another study there was no association between liver stiffness and presence of esophageal varices [79]. However in a recent study with three dimensional MRE [80] both hepatic and splenic stiffness were associated with esophageal varices and the performance of MRE was comparable to dynamic contrast enhanced imaging for predicting the presence of esophageal varices and high risk varices. Combined assessment of contrast enhanced imaging and MRE significantly increased the detection of varices of any grade compared to dynamic contrast enhanced imaging alone (85% vs. 74%) suggesting added value of MRE in patients with portal hypertension.

Compensated and decompensated liver cirrhosis

Patients with cirrhosis are further classified into compensated and decompensated cirrhosis based on the presence of variceal bleeding, ascites or hepatic encephalopathy. The outcome in decompensated liver cirrhosis is worse than in those with compensated liver cirrhosis [81]. In a meta-analysis study, Singh et al showed that liver stiffness measured with MRE is associated with increased risk of decompensation, development of hepatocellular carcinoma, and death [82].

In another study [83], MRE was independently associated with decompensation. In patients with compensated cirrhosis, the hazard for hepatic decompensation was 1.42 (95 % CI 1.16–1.75) per unit increase in liver shear stiffness over time. The hazard of hepatic decompensation was 4.96 (95 % CI 1.4–17.0, $p = 0.019$) for a subject with compensated disease and mean liver stiffness value 5.8 kPa as compared to an individual with compensated disease and lower mean liver stiffness values. These studies provide evidence for the role of MRE of the liver in prognostication and prediction of clinical outcomes in advanced fibrosis or cirrhosis.

Other applications of MRE in Liver

MRE of the liver may be useful in the follow up of chronic liver disease. Histological staging of liver fibrosis is not sensitive enough to detect minor changes in liver fibrosis amount or fibrosis progression, and change in histologic stage does not always reflect change in fibrosis burden as it involves subjective interpretation of anatomical changes and not an objective assessment of amount of fibrosis. Histology is therefore not suitable for monitoring therapies that are designed to stop or cause regression of fibrosis [84]. As MRE-measured liver stiffness correlates with fibrosis content [63] it may be useful in demonstrating progression or improvement of liver stiffness during clinical follow up (fig. 8).

MRE may be useful in the evaluation of focal liver lesions. Preliminary studies have indicated that malignant liver tumors have higher stiffness than benign tumors and normal liver [85, 86]. Future studies are awaited for confirmation of results from the preliminary studies and for possible clinical application in characterization of focal liver lesions.

MRE of liver transplants can also be performed and has been found useful in detection of advanced fibrosis in the liver transplants with recurrence of chronic liver disease [31, 87, 88]. MRE is also useful in the evaluation of congestive livers in post Fontan surgery patients for detection of liver fibrosis [89, 90]. Passively congested livers may be stiff without any fibrotic changes and therefore more studies of these patients with MRE is required to establish the correlation between congestion and liver stiffness.

Limitations of liver MRE

2D GRE-MRE is sensitive to the presence of iron in the liver and therefore MRE may technically fail in patients with high liver iron content. The presence of iron results in poor signal from the liver, but is not known to affect stiffness properties. The shear waves still travel through the liver but the signal from the liver is poor for a valid MRE. Newer sequences with low echo times that can improve liver signal have been developed and are useful in these livers [91]. Similar to other body MRI sequences, MRE may be limited in patients who are poor and inconsistent breath holders. Patients can be coached for breath holding for increased cooperation. One may also modify the MRE sequence, for example decreasing FOV as much as possible or reducing the matrix size (at the cost of resolution) to reduce the breath hold time and obtain a valid result.

MRE of Spleen

Splenomegaly is a common finding in patients with cirrhosis and non-cirrhotic portal hypertension and is probably due to increased portal venous pressure leading to congestion of blood in the spleen.

MRE of the spleen is best performed by placing the passive driver over the spleen, although propagation of the shear waves through the spleen can also be seen when MRE of the liver is performed [79, 92]. MRE performed with the passive driver over the spleen would ensure good propagation of shear waves through it resulting in reliable stiffness map generation.

Generally MRE of the spleen is also performed at the same acoustic frequency of 60Hz similar to liver. In earlier studies, splenic stiffness was found to correlate with splenic size, platelet count and presence of esophageal varices in patients with chronic liver disease [79, 93]. Spleen stiffness correlates with liver stiffness and, in patients with liver fibrosis, spleen stiffness increases in parallel with increasing liver stiffness [79]. A splenic stiffness greater than 10.5 kPa is predictive of esophageal varices (fig.9) suggesting the usefulness of splenic stiffness evaluation as a noninvasive method to assess portal hypertension. A large meta-analysis of studies on splenic stiffness measurement with ultrasound-based elastography techniques showed 78% sensitivity and 76% specificity for detection of any degree of esophageal varices based on pooled estimates, which is not accurate enough to support its use in routine clinical practice. There have been a limited number of large studies with MRE of the spleen, therefore the role of MRE of spleen for non-invasive prediction of esophageal varices is difficult to ascertain. Recently Shin et al. [38] using a 3D echo planar MRE technique demonstrated that both hepatic and splenic stiffness had positive linear correlations with the endoscopic grade of esophageal varices. In another study, spleen stiffness was found to have a significant correlation with the direct hepatic venous pressure gradient ($r^2=0.86$, $p<0.001$) [94]. Another study by Ronot et al [95] showed that spleen loss modulus was the best parameter for identifying patients with severe portal hypertension ($p = 0.019$, AUROC = 0.81) or high-risk varices ($p = 0.042$, AUROC = 0.93). Both studies suggest a promising role for MRE of the spleen in the evaluation of portal hypertension and significant esophageal varices

MRE of Pancreas

Chronic pancreatitis results in fibrosis of the gland, and adenocarcinoma of the pancreas is associated with a scirrhous tissue reaction. These processes may increase the stiffness of the pancreas and hence increased the interest in exploring the technique of MRE for evaluation of the pancreas.

The midline retroperitoneal location and small size of the pancreas poses a challenge to performing an MRE of this gland, however an initial study showed the feasibility of this technique [96]. Recently Shi et al [41] performed MRE in normal volunteers using a modified ergonomic flexible driver. As the gland is small, several modifications were needed to ensure a valid stiffness estimation. A three-dimensional (3D) spin-echo echo planar imaging (SE-EPI) MRE sequence operating at 40Hz was found to be the most suitable (fig.10). A direct inversion algorithm was also used to estimate tissue stiffness. As the pancreas is related to the stomach above, subjects for MRE should have an empty stomach so that the distance between the driver on the skin and the pancreas is reduced to ensure good wave propagation. This also would minimize any compression of the pancreas by a full stomach. The mean stiffness of a normal pancreas at 40Hz was 1.15 ± 0.17 kPa, and at 60Hz the stiffness was similar to a normal liver parenchyma.

The initial studies have shown the feasibility of performing MRE of the pancreas and results from studies evaluating its role in chronic pancreatitis and pancreatic cancers (fig.11) are eagerly awaited.

MRE of Kidneys

The retroperitoneal location of the kidneys poses challenges for the propagation of shear waves through them. In a preliminary study, the feasibility of MRE of the kidneys in healthy volunteers with subjects lying supine on an external driver was demonstrated [97]. It is also possible to design smaller drivers to be placed in contact with the back closer to the kidneys to ensure good propagation of shear waves and this is still under evaluation. In view of the small size of the kidneys, a higher frequency (90 Hz) and a 3D MRE technique similar to that described for MRE of the pancreas would be suitable. MRE studies can be obtained in various planes but the coronal plane including both kidneys would be useful for comparison (fig.12).

Renal stiffness is dependent on its tissue components. Kidneys are perfused richly with ~ 25% of the cardiac output. Nearly one fourth of the renal volume under normal physiological status can be attributed to blood pressure, blood within the kidneys, the glomerular filtrate within the tubules and urine [98]. Renal blood flow contributes significantly to the measured stiffness of the kidneys [99]. Anisotropy of the renal tissue may also impact on the stiffness evaluated in the kidney [100, 101]. The medulla is predominantly composed of tubular structures like vasa recta, collecting tubules and Henle loops that run from the capsule to the papilla making it highly anisotropic as compared to the cortex made of predominantly glomeruli and proximal tubules. Urinary obstruction may also influence the stiffness as it may increase the intra-renal pressure.

In a study with young healthy adults at 45Hz frequency, Rouviere et al [102] showed that MRE of the kidney was reproducible with an intra-subject variability of only 6%. In a recent study, high resolution MRE of the kidney was performed in nine healthy volunteers. In this study, the renal medulla was shown to have a higher stiffness than the cortex [103] which may be attributed to the complex tubular structure and more interstitium in the medulla. More definitive information on the regional variation of renal stiffness may be obtained with 3D MRE evaluation. Larger studies exploring the utility of MRE in chronic renal parenchymal disease are currently not available and are eagerly awaited.

Few studies have focused on MRE of the renal transplant. MRE of the renal transplant is technically easier to perform as renal transplants are usually located in the iliac fossa and therefore subject to less respiratory movement. They also are near to skin surface which facilitates better propagation of shear waves and less attenuation of high frequency shear waves (fig.13). In a preliminary study, a trend of increased stiffness in the transplants of patients with a mild or moderate degree of interstitial fibrosis was found with no significant differences [104]. In another preliminary study, higher stiffness was found in patients without interstitial fibrosis as compared to those with fibrosis [105]. The preliminary studies show a complex relationship between renal stiffness and the pathological processes in a renal transplant and needs to be further evaluated. MRE of renal transplants is another exciting area for future study and may be valuable in the evaluation of grafts in the future.

MRE of Uterus

The mechanical integrity of the uterine cervix is important for a successful pregnancy. Altered tissue structure may result in significant changes in the mechanical properties of the cervix and result in premature delivery. A non-invasive method to assess stiffness of the uterus and cervix may be useful in understanding mechanical factors affecting premature delivery and infertility. Knowledge of mechanical properties of normal uterus and cervix may also be useful in differentiation of focal lesions arising from these organs.

3D MRE of the uterus in healthy female volunteers showed that the uterine corpus had a higher elasticity but similar viscosity compared to cervix [106]. In this study, it was also found that stiffness of both endometrium and myometrium decreased during the menstrual cycle. More studies are required to confirm these preliminary findings.

Uterine fibroids or leiomyoma are common and frequently associated with pelvic symptoms and infertility. Fibroids have variable composition, and evaluation of the stiffness of the fibroids may give insights into their composition for treatment planning such as high-frequency ultrasound (HiFU). Mechanotransduction is thought to be a significant factor affecting the growth of uterine fibroids. Stiffness of fibroids may contribute to their growth [107] and possibly their recurrence.

In a preliminary study, Stewart et al [108] performed MRE of the uterus in a supine position with the passive driver placed on the lower abdomen overlying the uterus. A 2D-GRE MRE sequence at 60Hz acoustic frequency similar to that of liver MRE was used (fig.14). They demonstrated variable stiffness of the fibroids that probably represents different composition of the fibroids. However this was not histologically correlated and future studies in this direction are required. The fibroids studied had an average stiffness of 5.09kPa (range, 3.95 to 6.68kPa). The size of the fibroids studied was in the range of 4.5 to 22.5cm. Evaluation of tiny fibroids may be best done with a 3D MRE sequence. In another study, Hesley et al [109] showed that fibroids became stiffer after HiFU. Results from these preliminary studies are encouraging and provide motivation for future studies on stiffness of uterine fibroids and its correlation with histological findings for characterization of the fibroids. Assessment of mechanical properties of uterine fibroids may be useful for prediction of their growth and predicting treatment outcomes.

MRE of other abdominal organs

Successful clinical application of MRE of the liver and its increasing utility has stirred interest in evaluation of other abdominal organs. Evaluation of prostate via transrectal and transperineal approaches has been described [110, 111]. Other organs to be explored include bowel and urinary bladder. These organs are technically challenging owing to their location, mobility, physiological motion and/or small size of tissue (wall thickness) to be studied. However newer innovations in MRE may soon make it possible to evaluate these organs.

References

1. Fung YC, Liu SQ. Elementary mechanics of the endothelium of blood vessels. *J Biomech Eng.* 1993; 115:1–12. [PubMed: 8445886]
2. GIERKE HE, OESTREICHER HL, FRANKE EK, PARRACK HO, WITTERN WW. Physics of vibrations in living tissues. *J Appl Physiol.* 1952; 4:886–900. [PubMed: 14946086]
3. Manduca A, Oliphant T, Dresner M, et al. Magnetic resonance elastography: non-invasive mapping of tissue elasticity. *Med Image Anal.* 2001; 5:237–254. [PubMed: 11731304]
4. Oliphant TE, Manduca A, Ehman RL, Greenleaf JF. Complex-valued stiffness reconstruction for magnetic resonance elastography by algebraic inversion of the differential equation. *Magn Reson Med.* 2001; 45:299–310. [PubMed: 11180438]
5. Sarvazyan AP. Acoustic properties of tissues relevant to therapeutic applications. *Br J Cancer Suppl.* 1982; 5:52–54. [PubMed: 6950774]
6. Sarvazyan, AP.; Skovoroda, AR.; Emelianov, SY., et al. Biophysical Bases of Elasticity Imaging.. In: Jones, JP., editor. *Acoustical Imaging.* Plenum Press; New York: 1995. p. 223-240.
7. Sarvazyan AP, Rudenko OV, Swanson SD, Fowlkes JB, Emelianov SY. Shear wave elasticity imaging: A new ultrasonic technology of medical diagnostics. *Ultrasound in Medicine and Biology.* 1998; 24:1419–1435. [PubMed: 10385964]
8. Sarvazyan A, Hall TJ, Urban MW, Fatemi M, Aglyamov SR, Garra BS. An overview of elastography-an emerging branch of medical imaging. *Current Medical Imaging Reviews.* 2011; 7:255–282. [PubMed: 22308105]
9. Sarvazyan AP, Urban MW, Greenleaf JF. Acoustic waves in medical imaging and diagnostics. *Ultrasound Med Biol.* 2013; 39:1133–1146. [PubMed: 23643056]
10. Wilson LS, Robinson DE, Dadd MJ. Elastography - the movement begins. *Physics in Medicine and Biology.* 2000; 45:1409–1421. [PubMed: 10870700]
11. Gao L, Parker KJ, Lerner RM, Levinson SF. Imaging of the elastic properties of tissue - A review. *Ultrasound in Medicine and Biology.* 1996; 22:959–977. [PubMed: 9004420]
12. Greenleaf JF, Muthupillai R, Rossman PJ, Lomas DJ, Riederer SJ, Ehman RL. Measurement of tissue elasticity using magnetic resonance elastography. *Review of Progress in Quantitative Nondestructive Evaluation.* 1997; 16:19–26.
13. Greenleaf JF, Fatemi M, Insana M. Selected methods for imaging elastic properties of biological tissues. *Annual Review of Biomedical Engineering.* 2003; 5:57–78.
14. Muthupillai R, Lomas D, Rossman P, Greenleaf J, Manduca A, Ehman R. Magnetic resonance elastography by direct visualization of propagating acoustic strain waves. *Science.* 1995; 269:1854–1857. [PubMed: 7569924]
15. Mariappan YK, Glaser KJ, Ehman RL. Magnetic resonance elastography: a review. *Clin Anat.* 2010; 23:497–511. [PubMed: 20544947]
16. Glaser KJ, Manduca A, Ehman RL. Review of MR elastography applications and recent developments. *J Magn Reson Imaging.* 2012; 36 spcone.
17. Sandrin L, Fourquet B, Hasquenoph JM, et al. Transient elastography: a new noninvasive method for assessment of hepatic fibrosis. *Ultrasound Med Biol.* 2003; 29:1705–1713. [PubMed: 14698338]
18. de Ledinghen V, Douvin C, Kettaneh A, et al. Diagnosis of hepatic fibrosis and cirrhosis by transient elastography in HIV/hepatitis C virus-coinfected patients. *J Acquir Immune Defic Syndr.* 2006; 41:175–179. [PubMed: 16394849]
19. Talwalkar J, Kurtz D, Schoenleber S, West C, Montori V. Ultrasound-based transient elastography for the detection of hepatic fibrosis: systematic review and meta-analysis. *Clin Gastroenterol Hepatol.* 2007; 5:1214–1220. [PubMed: 17916549]
20. Friedrich-Rust M, Ong MF, Martens S, et al. Performance of transient elastography for the staging of liver fibrosis: a meta-analysis. *Gastroenterology.* 2008; 134:960–974. [PubMed: 18395077]
21. Castera L. Invasive and non-invasive methods for the assessment of fibrosis and disease progression in chronic liver disease. *Best Pract Res Clin Gastroenterol.* 2011; 25:291–303. [PubMed: 21497746]

22. Venkatesh SK, Wang G, Teo LLS, Ang BWL. Magnetic Resonance Elastography of Liver in Healthy Asians: Normal Liver Stiffness Quantification and Reproducibility Assessment. *Journal of Magnetic Resonance Imaging*. 2013
23. Ichikawa S, Motosugi U, Ichikawa T, et al. Magnetic resonance elastography for staging liver fibrosis in chronic hepatitis C. *Magn Reson Med Sci*. 2012; 11:291–297. [PubMed: 23269016]
24. Venkatesh SK, Wang G, Lim SG, Wee A. Magnetic resonance elastography for the detection and staging of liver fibrosis in chronic hepatitis B. *Eur Radiol*. 2014; 24:70–78. [PubMed: 23928932]
25. Yin M, Talwalkar J, Glaser K, et al. Assessment of hepatic fibrosis with magnetic resonance elastography. *Clin Gastroenterol Hepatol*. 2007; 5:1207–1213. e1202. [PubMed: 17916548]
26. Huwart L, Peeters F, Sinkus R, et al. Liver fibrosis: non-invasive assessment with MR elastography. *Nmr in Biomedicine*. 2006; 19:173–179. [PubMed: 16521091]
27. Huwart L, Sempoux C, Salameh N, et al. Liver fibrosis: Noninvasive assessment with MR elastography versus aspartate aminotransferase-to-platelet ratio index. *Radiology*. 2007; 245:458–466. [PubMed: 17940304]
28. Huwart L, Sempoux C, Vicaut E, et al. Magnetic resonance elastography for the noninvasive staging of liver fibrosis. *Gastroenterology*. 2008; 135:32–40. [PubMed: 18471441]
29. Huwart L, Salameh N, ter Beek LC, et al. MR elastography of liver fibrosis: preliminary results comparing spin-echo and echo-planar imaging. *European Radiology*. 2008; 18:2535–2541. [PubMed: 18504591]
30. Kim BH, Lee JM, Lee YJ, et al. MR elastography for noninvasive assessment of hepatic fibrosis: experience from a tertiary center in Asia. *J Magn Reson Imaging*. 2011; 34:1110–1116. [PubMed: 21932355]
31. Lee VS, Miller FH, Omary RA, et al. Magnetic resonance elastography and biomarkers to assess fibrosis from recurrent hepatitis C in liver transplant recipients. *Transplantation*. 2011; 92:581–586. [PubMed: 21822174]
32. Lee DH, Lee JM, Han JK, Choi BI. MR elastography of healthy liver parenchyma: Normal value and reliability of the liver stiffness value measurement. *J Magn Reson Imaging*. 2012
33. Lee YJ, Lee JM, Lee JE, et al. MR elastography for noninvasive assessment of hepatic fibrosis: Reproducibility of the examination and reproducibility and repeatability of the liver stiffness value measurement. *J Magn Reson Imaging*. 2013
34. Hines CDG, Bley TA, Lindstrom MJ, Reeder SB. Repeatability of magnetic resonance elastography for quantification of hepatic stiffness. *Journal of Magnetic Resonance Imaging*. 2010; 31:725–731. [PubMed: 20187219]
35. Asbach P, Klatt D, Schlosser B, et al. Viscoelasticity-based staging of hepatic fibrosis with multifrequency MR elastography. *Radiology*. 2010; 257:80–86. [PubMed: 20679447]
36. Asbach P, Klatt D, Hamhaber U, et al. Assessment of liver viscoelasticity using multifrequency MR elastography. *Magn Reson Med*. 2008; 60:373–379. [PubMed: 18666132]
37. Rouviere O, Yin M, Dresner MA, et al. MR elastography of the liver: preliminary results. *Radiology*. 2006; 240:440–448. [PubMed: 16864671]
38. Huwart L, Peeters F, Sinkus R, et al. Liver fibrosis: non-invasive assessment with MR elastography. *NMR Biomed*. 2006; 19:173–179. [PubMed: 16521091]
39. Klatt D, Asbach P, Rump J, et al. In vivo determination of hepatic stiffness using steady-state free precision magnetic resonance elastography. *Investigative Radiology*. 2006; 41:841–848. [PubMed: 17099421]
40. Chen, J.; Stanley, D.; Glaser, K.; Yin, M.; Rossman, P.; Ehman, R. Ergonomic Flexible Drivers for Hepatic MR Elastography.. Annual Meeting of International Society for Magnetic Resonance in Medicine; Stockholm, Sweden. 2010;
41. Shi Y, Glaser KJ, Venkatesh SK, Ben-Abraham EI, Ehman RL. Feasibility of using 3D MR elastography to determine pancreatic stiffness in healthy volunteers. *J Magn Reson Imaging*. 2014
42. Muthupillai R, Lomas DJ, Rossman PJ, et al. Visualizing propagating transverse mechanical waves in tissue-like media using magnetic resonance imaging. *Acoustical Imaging*. 1996; 22:279–283.
43. Rump J, Klatt D, Braun J, Warmuth C, Sack I. Fractional encoding of harmonic motions in MR elastography. *Magn Reson Med*. 2007; 57:388–395. [PubMed: 17260354]

44. Glaser KJ, Felmlee JP, Ehman RL. Rapid MR elastography using selective excitation. *Magnetic Resonance in Medicine*. 2006; 55:1381–1389. [PubMed: 16683257]
45. Manduca A, Dutt V, Borup DT, Muthupillai R, Greenleaf JF, Ehman RL. An inverse approach to the calculation of elasticity maps for magnetic resonance elastography. *Medical Imaging: Image Processing, SPIE*. 1998; 3338:426–436.
46. Manduca A, Lake D, Kruse S, Ehman R. Spatio-temporal directional filtering for improved inversion of MR elastography images. *Med Image Anal*. 2003; 7:465–473. [PubMed: 14561551]
47. Chen Q, Ringleb SI, Manduca A, Ehman RL, An KN. A finite element model for analyzing shear wave propagation observed in magnetic resonance elastography. *Journal of Biomechanics*. 2005; 38:2198–2203. [PubMed: 16154406]
48. Chen Q, Ringleb SI, Manduca A, Ehman RL, An KN. Differential effects of pre-tension on shear wave propagation in elastic media with different boundary conditions as measured by magnetic resonance elastography and finite element modeling. *Journal of Biomechanics*. 2006; 39:1428–1434. [PubMed: 15964007]
49. Huwart L, Sempoux C, Vicaut E, et al. Magnetic resonance elastography for the noninvasive staging of liver fibrosis. *Gastroenterology*. 2008; 135:32–40. [PubMed: 18471441]
50. Venkatesh SK, Yin M, Ehman RL. Magnetic resonance elastography of liver: clinical applications. *J Comput Assist Tomogr*. 2013; 37:887–896. [PubMed: 24270110]
51. Venkatesh SK, Yin M, Ehman RL. Magnetic resonance elastography of liver: technique, analysis, and clinical applications. *J Magn Reson Imaging*. 2013; 37:544–555. [PubMed: 23423795]
52. Godfrey EM, Patterson AJ, Priest AN, et al. A comparison of MR elastography and P-31 MR spectroscopy with histological staging of liver fibrosis. *European Radiology*. 2012; 22:2790–2797. [PubMed: 22752441]
53. Yin M, Talwalkar JA, Glaser KJ, et al. Dynamic postprandial hepatic stiffness augmentation assessed with MR elastography in patients with chronic liver disease. *AJR Am J Roentgenol*. 2011; 197:64–70. [PubMed: 21701012]
54. Hines CDG, Lindstrom MJ, Varma AK, Reeder SB. Effects of postprandial state and mesenteric blood flow on the repeatability of MR elastography in asymptomatic subjects. *Journal of Magnetic Resonance Imaging*. 2011; 33:239–244. [PubMed: 21182146]
55. Motosugi U, Ichikawa T, Sou H, et al. Effects of gadoxetic acid on liver elasticity measurement by using magnetic resonance elastography. *Magn Reson Imaging*. 2012; 30:128–132. [PubMed: 21937180]
56. Hallinan JT, Alsaf HS, Wee A, Venkatesh SK. Magnetic Resonance Elastography of Liver: Influence of Intravenous Gadolinium Administration on Measured Liver Stiffness. *Abdom Imaging*. 2014
57. Dzyubak B, Glaser K, Yin M, et al. Automated liver stiffness measurements with magnetic resonance elastography. *Journal of magnetic resonance imaging : JMRI*. 2013; 38:371–379. [PubMed: 23281171]
58. Motosugi U, Ichikawa T, Sano K, et al. Magnetic resonance elastography of the liver: preliminary results and estimation of inter-rater reliability. *Jpn J Radiol*. 2010; 28:623–627. [PubMed: 20972864]
59. Runge JH, Bohte AE, Verheij J, et al. Comparison of interobserver agreement of magnetic resonance elastography with histopathological staging of liver fibrosis. *Abdom Imaging*. 2013
60. Venkatesh SK, Wang G, Teo LL, Ang BW. Magnetic resonance elastography of liver in healthy asians: normal liver stiffness quantification and reproducibility assessment. *J Magn Reson Imaging*. 2014; 39:1–8. [PubMed: 24123300]
61. Caballero T, Pérez-Milena A, Masseroli M, et al. Liver fibrosis assessment with semiquantitative indexes and image analysis quantification in sustained-responder and non-responder interferon-treated patients with chronic hepatitis C. *J Hepatol*. 2001; 34:740–747. [PubMed: 11434621]
62. Lazzarini AL, Levine RA, Ploutz-Snyder RJ, Sanderson SO. Advances in digital quantification technique enhance discrimination between mild and advanced liver fibrosis in chronic hepatitis C. *Liver Int*. 2005; 25:1142–1149. [PubMed: 16343064]
63. Venkatesh SK, Xu S, Tai D, Yu H, Wee A. Correlation of MR elastography with morphometric quantification of liver fibrosis (Fibro-C-Index) in chronic hepatitis B. *Magn Reson Med*. 2013

64. Huwart L, Sempoux C, Salameh N, et al. Liver fibrosis: noninvasive assessment with MR elastography versus aspartate aminotransferase-to-platelet ratio index. *Radiology*. 2007; 245:458–466. [PubMed: 17940304]
65. Venkatesh, SK.; Takahashi, N.; Glocker, JF., et al. Non-invasive Diagnosis of Liver Fibrosis: Conventional MR Imaging Findings versus MR Elastography.. Proceedings of 17th annual meeting of ISMRM; Toronto. 2008; Toronto: ISMRM; 2008. (abstract 2613)
66. Venkatesh SK, Ehman RL. Magnetic Resonance Elastography of Liver. *Magn Reson Imaging Clin N Am*. 2014; 22:433–446. [PubMed: 25086938]
67. Shi Y, Guo Q, Xia F, et al. MR elastography for the assessment of hepatic fibrosis in patients with chronic hepatitis B infection: does histologic necroinflammation influence the measurement of hepatic stiffness? *Radiology*. 2014; 273:88–98. [PubMed: 24893048]
68. Ichikawa S, Motosugi U, Nakazawa T, et al. Hepatitis activity should be considered a confounder of liver stiffness measured with MR elastography. *J Magn Reson Imaging*. 2014
69. Younossi ZM, Stepanova M, Afendy M, et al. Changes in the prevalence of the most common causes of chronic liver diseases in the United States from 1988 to 2008. *Clin Gastroenterol Hepatol*. 2011; 9:524–530. e521. quiz e560. [PubMed: 21440669]
70. Williams CD, Stengel J, Asike MI, et al. Prevalence of nonalcoholic fatty liver disease and nonalcoholic steatohepatitis among a largely middle-aged population utilizing ultrasound and liver biopsy: a prospective study. *Gastroenterology*. 2011; 140:124–131. [PubMed: 20858492]
71. Welsh JA, Karpen S, Vos MB. Increasing prevalence of nonalcoholic fatty liver disease among United States adolescents, 1988-1994 to 2007-2010. *J Pediatr*. 2013; 162:496–500. e491. [PubMed: 23084707]
72. Chen J, Talwalkar JA, Yin M, Glaser KJ, Sanderson SO, Ehman RL. Early detection of nonalcoholic steatohepatitis in patients with nonalcoholic fatty liver disease by using MR elastography. *Radiology*. 2011; 259:749–756. [PubMed: 21460032]
73. Kim D, Kim WR, Talwalkar JA, Kim HJ, Ehman RL. Advanced fibrosis in nonalcoholic fatty liver disease: noninvasive assessment with MR elastography. *Radiology*. 2013; 268:411–419. [PubMed: 23564711]
74. Loomba R, Wolfson T, Ang B, et al. Magnetic resonance elastography predicts advanced fibrosis in patients with nonalcoholic fatty liver disease: A prospective study. *Hepatology*. 2014
75. Venkatesh SK, Reeder SB. New and improved imaging modalities for NAFLD. *Current Hepatology Reports*. 2014; 13:9.
76. Vizzutti F, Arena U, Romanelli RG, et al. Liver stiffness measurement predicts severe portal hypertension in patients with HCV-related cirrhosis. *Hepatology*. 2007; 45:1290–1297. [PubMed: 17464971]
77. Lim JK, Groszmann RJ. Transient elastography for diagnosis of portal hypertension in liver cirrhosis: is there still a role for hepatic venous pressure gradient measurement? *Hepatology*. 2007; 45:1087–1090. [PubMed: 17464984]
78. Sun HY, Lee JM, Han JK, Choi BI. Usefulness of MR elastography for predicting esophageal varices in cirrhotic patients. *J Magn Reson Imaging*. 2014; 39:559–566. [PubMed: 24115368]
79. Talwalkar JA, Yin M, Venkatesh SK, et al. Feasibility of in vivo MR elastographic splenic stiffness measurements in the assessment of portal hypertension. *American Journal of Roentgenology*. 2009; 193:122–127. [PubMed: 19542403]
80. Shin SU, Lee JM, Yu MH, et al. Prediction of Esophageal Varices in Patients with Cirrhosis: Usefulness of Three-dimensional MR Elastography with Echo-planar Imaging Technique. *Radiology*. 2014:130916.
81. Fleming KM, Aithal GP, Card TR, West J. All-cause mortality in people with cirrhosis compared with the general population: a population-based cohort study. *Liver Int*. 2012; 32:79–84. [PubMed: 21745279]
82. Singh S, Fujii LL, Murad MH, et al. Liver stiffness is associated with risk of decompensation, liver cancer, and death in patients with chronic liver diseases: a systematic review and meta-analysis. *Clin Gastroenterol Hepatol*. 2013; 11:1573–1584. e1571–1572. quiz e1588-1579. [PubMed: 23954643]

83. Asrani SK, Talwalkar JA, Kamath PS, et al. Role of magnetic resonance elastography in compensated and decompensated liver disease. *J Hepatol.* 2014; 60:934–939. [PubMed: 24362072]
84. O'Brien MJ, Keating NM, Elderiny S, et al. An assessment of digital image analysis to measure fibrosis in liver biopsy specimens of patients with chronic hepatitis C. *Am J Clin Pathol.* 2000; 114:712–718. [PubMed: 11068544]
85. Venkatesh S, Yin M, Glockner J, et al. MR elastography of liver tumors: preliminary results. *AJR Am J Roentgenol.* 2008; 190:1534–1540. [PubMed: 18492904]
86. Garteiser P, Doblaz S, Daire JL, et al. MR elastography of liver tumours: value of viscoelastic properties for tumour characterisation. *Eur Radiol.* 2012; 22:2169–2177. [PubMed: 22572989]
87. Crespo S, Bridges M, Nakhleh R, McPhail A, Pungpapong S, Keaveny AP. Non-invasive assessment of liver fibrosis using magnetic resonance elastography in liver transplant recipients with hepatitis C. *Clin Transplant.* 2013; 27:652–658. [PubMed: 23837611]
88. Kamphues C, Klatt D, Bova R, et al. Viscoelasticity-based magnetic resonance elastography for the assessment of liver fibrosis in hepatitis C patients after liver transplantation. *Rofo.* 2012; 184:1013–1019. [PubMed: 22893489]
89. Serai SD, Wallihan DB, Venkatesh SK, et al. Magnetic Resonance Elastography of the Liver in Patients Status-Post Fontan Procedure: Feasibility and Preliminary Results. *Congenit Heart Dis.* 2013
90. Serai, sD; Wallihan, DB.; Venkatesh sk, Ehman RL.; Podberesky, DJ. MR Elastography of the liver in patients status post Fontan procedure: A pilot investigation.. *Proceedings of 21st Annual ISMRM Conference; Salt Lake City, UT.* 2013; (abstract 3361)
91. Mariappan, YK.; Venkatesh, SK.; Glaser, JK.; McGee, KP.; Ehman, RL. MR Elastography of liver with iron overload: development, evaluation and preliminary clinical experience with improved spin echo and spin echo EPI sequences.. *The 21st Annual Conference of International Society for Magnetic Resonance in Medicine; Salt Lake City, Utah.* 2013; p. 278
92. Mannelli L, Godfrey E, Joubert I, et al. MR elastography: spleen stiffness measurements in healthy volunteers-preliminary experience. *American Journal of Roentgenology.* 2010; 195:387–392. [PubMed: 20651194]
93. Morisaka H, Motosugi U, Ichikawa S, Sano K, Ichikawa T, Enomoto N. Association of splenic MR elastographic findings with gastroesophageal varices in patients with chronic liver disease. *J Magn Reson Imaging.* 2013
94. Nedredal GI, Yin M, McKenzie T, et al. Portal hypertension correlates with splenic stiffness as measured with MR elastography. *Journal of Magnetic Resonance Imaging.* 2011; 34:79–87. [PubMed: 21608066]
95. Ronot M, Lambert S, Elkrief L, et al. Assessment of portal hypertension and high-risk oesophageal varices with liver and spleen three-dimensional multifrequency MR elastography in liver cirrhosis. *Eur Radiol.* 2014; 24:1394–1402. [PubMed: 24626745]
96. Yin, M.; Venkatesh, SK.; Grimm, RC.; Rossman, PJ.; Manduca, A.; Ehman, RL. Assessment of the pancreas with MR elastography.. *Proceedings of the International Society for Magnetic Resonance in Medicine; Toronto, Canada.* 2008; p. 2627
97. Venkatesh, SK.; Yin, M.; Grimm, RC.; Rossman, P.; Ehman, RL. MR Elastography of the kidneys: preliminary results.. *16th Annual Meeting ISMRM; Toronto.* 2008; p. 461
98. Lerman LO, Bentley MD, Bell MR, Rumberger JA, Romero JC. Quantitation of the in vivo kidney volume with cine computed tomography. *Invest Radiol.* 1990; 25:1206–1211. [PubMed: 2254054]
99. Warner L, Yin M, Glaser KJ, et al. Noninvasive In Vivo Assessment of Renal Tissue Elasticity During Graded Renal Ischemia Using MR Elastography. *Invest Radiol.* 2011; 46:509–514. [PubMed: 21467945]
100. Gennisson JL, Grenier N, Combe C, Tanter M. Supersonic shear wave elastography of in vivo pig kidney: influence of blood pressure, urinary pressure and tissue anisotropy. *Ultrasound Med Biol.* 2012; 38:1559–1567. [PubMed: 22698515]
101. Grenier N, Poulain S, Lepreux S, et al. Quantitative elastography of renal transplants using supersonic shear imaging: a pilot study. *Eur Radiol.* 2012; 22:2138–2146. [PubMed: 22588518]

102. Rouviere O, Souchon R, Pagnoux G, Menager J-M, Chapelon JY. Magnetic resonance elastography of the kidneys: feasibility and reproducibility in young healthy adults. *Journal of Magnetic Resonance Imaging*. 2011; 34:880–886. [PubMed: 21769970]
103. Streitberger KJ, Guo J, Tzschätzsch H, et al. High-resolution mechanical imaging of the kidney. *J Biomech*. 2014; 47:639–644. [PubMed: 24355382]
104. Lee CU, Glockner JF, Glaser KJ, et al. MR elastography in renal transplant patients and correlation with renal allograft biopsy: a feasibility study. *Acad Radiol*. 2012; 19:834–841. [PubMed: 22503893]
105. Venkatesh, SK.; Wang, G.; Thamboo, TP.; Liu, E.; Siew, EPY.; Anantram, V. MR Elastography of Renal Transplants: Correlating stiffness with Interstitial fibrosis and Tubular Atrophy.. *Proceedings of 20th Annual Meeting ISMRM; Melbourne*. 2012; p. 4062
106. Jiang X, Asbach P, Streitberger KJ, et al. In vivo high-resolution magnetic resonance elastography of the uterine corpus and cervix. *Eur Radiol*. 2014; 24:3025–3033. [PubMed: 25038856]
107. Norian JM, Owen CM, Taboas J, et al. Characterization of tissue biomechanics and mechanical signaling in uterine leiomyoma. *Matrix Biol*. 2012; 31:57–65. [PubMed: 21983114]
108. Stewart EA, Taran FA, Chen J, et al. Magnetic resonance elastography of uterine leiomyomas: a feasibility study. *Fertil Steril*. 2011; 95:281–284. [PubMed: 20633880]
109. Gina H, K G, D W. MRE following focused ultrasound treatment of uterine fibroids. In: *Focused ultrasound therapy-2nd European Symposium*. Rome. 2013
110. Arani A, Da Rosa M, Ramsay E, Plewes DB, Haider MA, Chopra R. Incorporating endorectal MR elastography into multi-parametric MRI for prostate cancer imaging: Initial feasibility in volunteers. *J Magn Reson Imaging*. 2013
111. Sahebjavaher RS, Baghani A, Honarvar M, Sinkus R, Salcudean SE. Transperineal prostate MR elastography: initial in vivo results. *Magnetic Resonance in Medicine*. 2013; 69:411–420. [PubMed: 22505273]

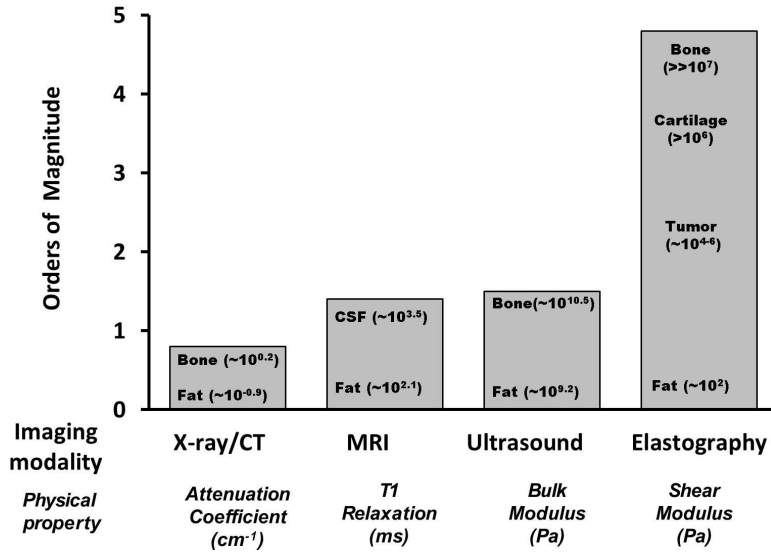


Fig.1. Bar chart showing different imaging modalities and the spectrum of contrast mechanisms utilized by them are shown. The shear modulus has the largest variation (more than five orders) of magnitude among various physiological states of normal and pathologic tissues. [Adapted with permission from Mariappan et al *Clin Anat* ; 23:497-511 (ref.15)].

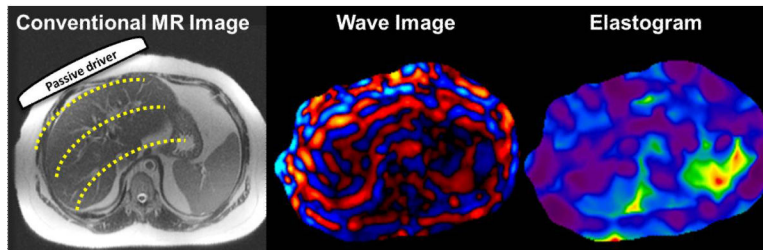


Fig.2.

Basic principles of magnetic resonance elastography illustrated here with an example of liver MRE. A passive driver is placed over the right lobe of the liver which transmits the acoustic vibrations from active driver into the abdomen. These vibrations generate mechanical shear waves (yellow dotted lines) (a). Wave image (b) obtained from a 2D-GRE-MRE sequence with motion encoding gradients synchronized with the active mechanical driver and giving a snapshot of the propagating shear waves. From the wave information, an automatic inversion algorithm produces a stiffness map.

Passive drivers and their positioning for abdominal MRE

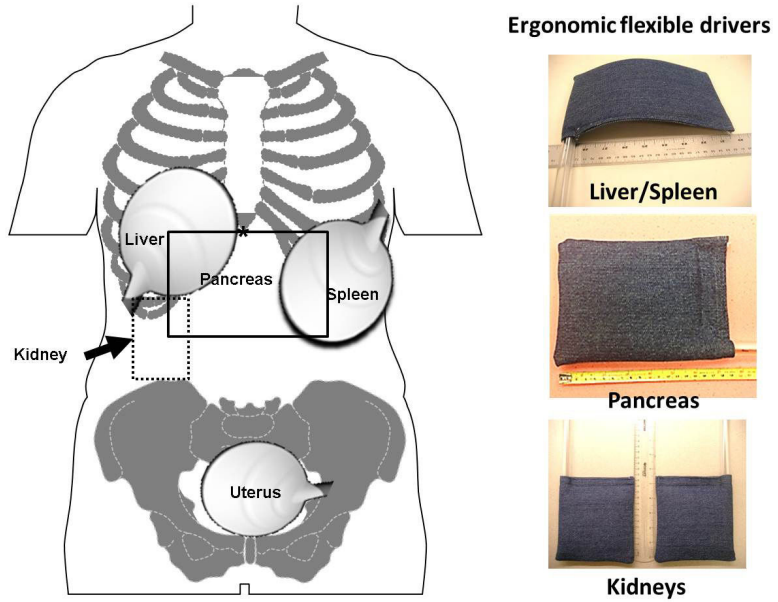


Fig.3. Diagram showing placement of the passive drivers for MRE of the liver, pancreas, spleen, kidney and uterus. Note for MRE of the liver, the driver is placed at the level of xiphisternum (*) and the driver for the kidney is placed on the back. Ergonomic flexible drivers that can be used for MRE of the liver/spleen, pancreas and the kidneys are shown (inset).

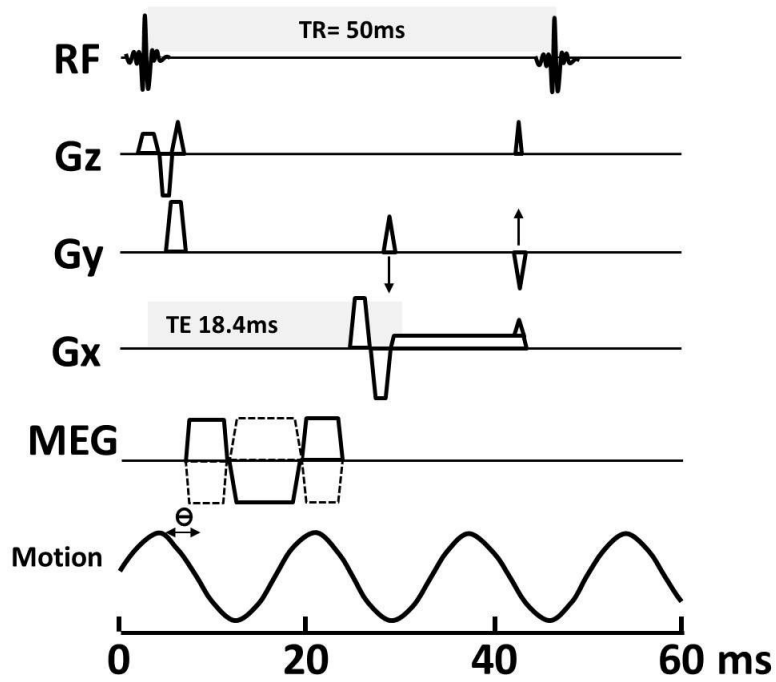


Fig 4.

Schematic diagram of a 2D GRE MRE pulse sequence. The TR (time to repeat) and TE (time to echo) in this illustration is 50ms and 18.4ms respectively. Motion encoding gradients (MEGs) are synchronized with the applied vibration throughout image acquisition. The MEGs can be applied to sensitize the sequence to cyclic tissue motion in any of the x, y, or z directions, as shown. The phase relationship (Θ) between the MEGs and the acoustic waves can be adjusted in steps to acquire wave images at different phases of the cyclic motion. Note that TE is variable and illustrated here is a TE of 18.4 so that signal is in the in-phase and gives maximum signal from the liver.

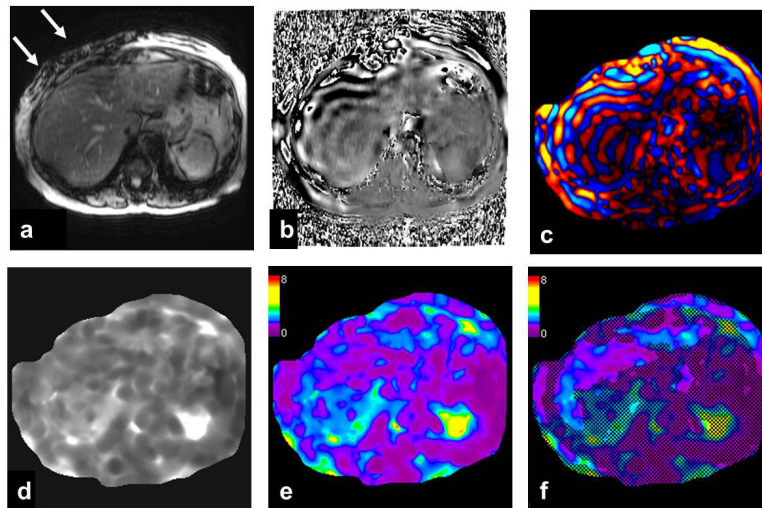


Fig.5.

An example of 2D-GRE-MRE sequence of the liver with raw data and processed images from inversion algorithm. Images from a single MRE slice through the liver produces raw magnitude (a) and (b) phase images. Note the signal loss due to intravoxel phase dispersion induced by acoustic waves (white arrow) produced by the driver opposed to the abdominal wall. Wave image (c) in color showing traversing shear waves through the cross-section of the abdomen. Gray scale stiffness map (d) on which regions of interest can be drawn to measure tissue stiffness. Color stiffness map with color scale of 0 to 8 kilo pascals (e) useful for a qualitative assessment. Confidence map (f) showing areas with less reliable stiffness (<95%) crossed out. Regions of interest should be drawn within the region not crossed out for valid stiffness measurement.

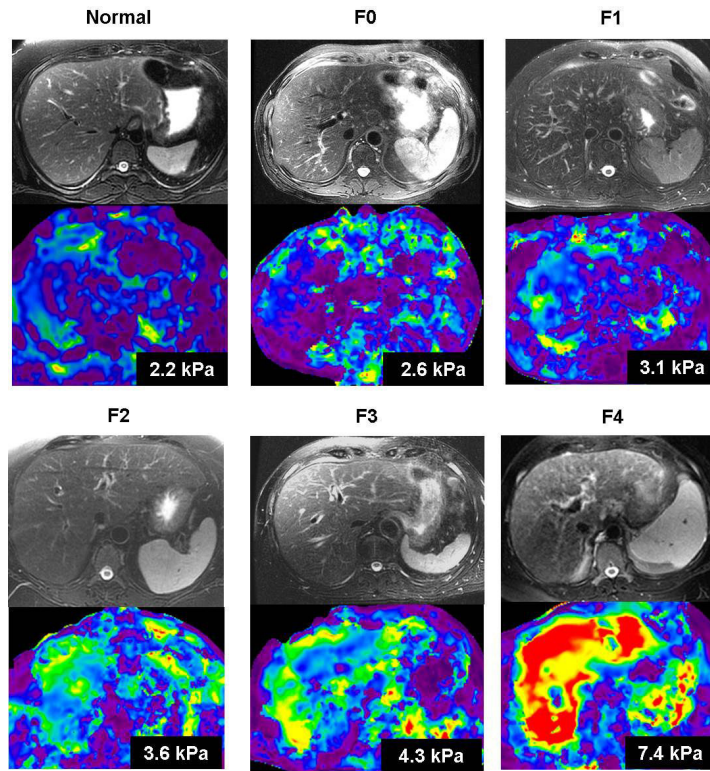


Fig.6. Liver stiffness increases with increasing fibrosis stage. Axial fat suppressed T2 weighted images and stiffness maps from a normal healthy volunteer and five different chronic hepatitis C patients with biopsy confirmed fibrosis (METAVIR stages F0 through F4). The numbers on stiffness maps are mean liver stiffness.

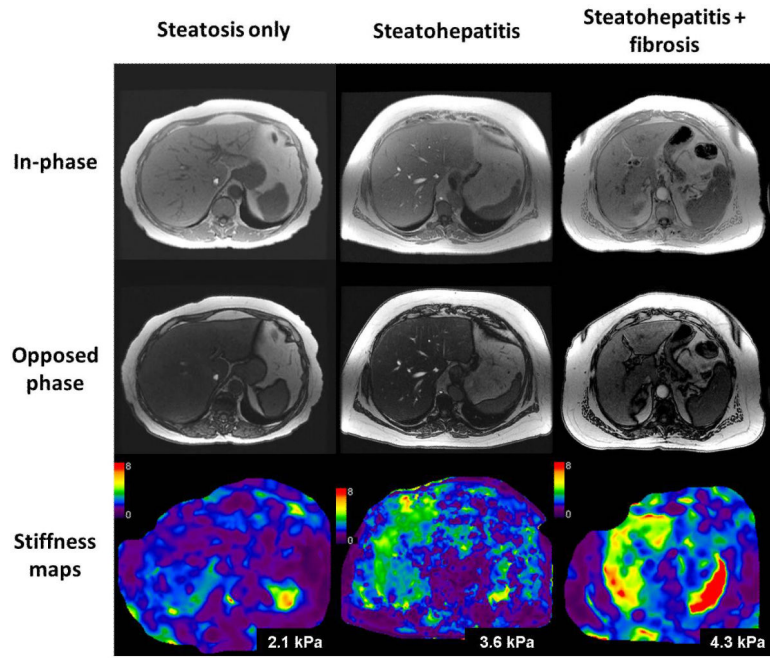
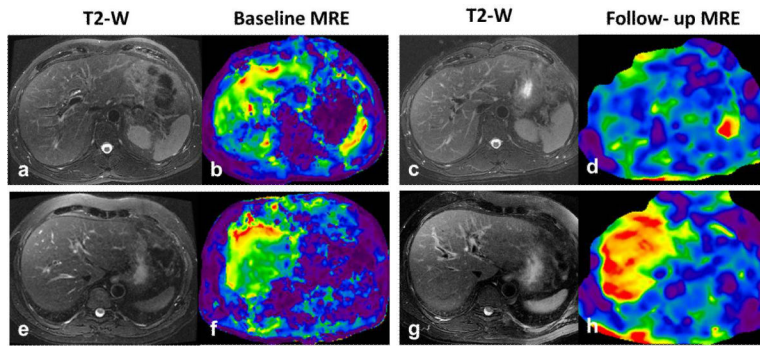


Fig.7. Utility of MRE in the evaluation of non alcoholic fatty liver disease (NAFLD). Examples of patients with biopsy proven simple steatosis (first column), non alcoholic steatohepatitis (second column), and steatohepatitis with fibrosis (third column). In-phase (top row), opposed phase (middle row) images from fast gradient sequence and stiffness maps (bottom row). The mean liver stiffness was 2.1, 3.6 and 4.3kPa respectively.

**Fig.8.**

Utility of liver MRE in longitudinal clinical follow up. Top row (a-d) -A case of chronic hepatitis C with baseline liver stiffness of 4.2kPa (b) and a follow up MRE after 3 years following antiviral treatment showed reduced liver stiffness to 2.8kPa suggestive of response to treatment. Bottom row (e-h)-Another case of chronic hepatitis C with a baseline liver stiffness of 4.2kPa who showed progression of disease with liver stiffness increasing to 6.3kPa within one year. This patient later developed portal hypertension on follow up with stiffness increasing to 9.2kPa after 3 years (not shown). Note there are no significant morphological changes in liver on the T2-w images for both cases.

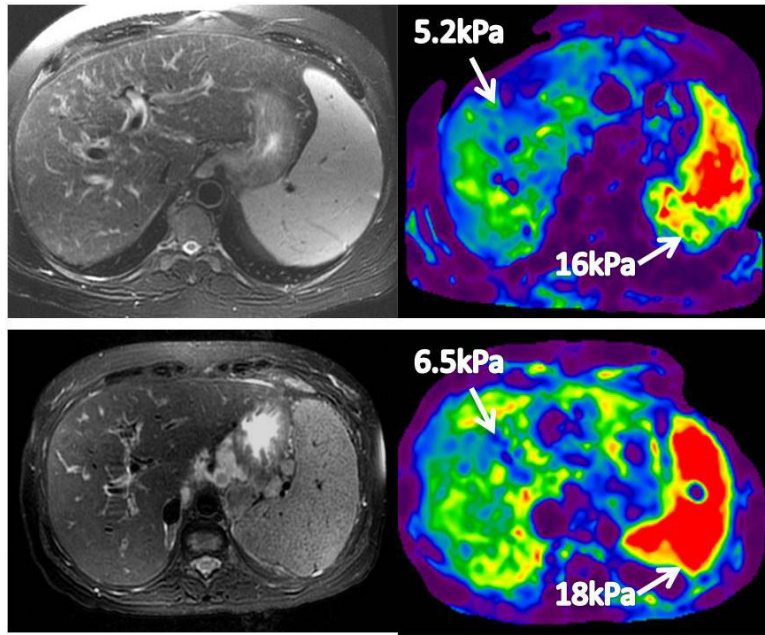


Fig.9. MRE of the spleen. Top row- A patient with chronic hepatitis C cirrhosis with portal gastropathy and esophageal varices. Bottom row –Another patient with cryptogenic cirrhosis with portal hypertension, esophageal varices and ascites. In both cases, the splenic stiffness is more than 10kPa.

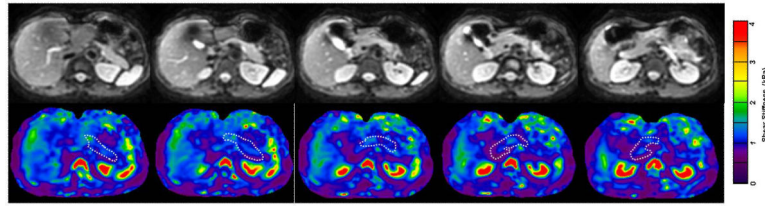


Fig.10. MRE of normal pancreas with 3D-EPI MRE technique performed at 40Hz. Magnitude images (top row) and stiffness maps (bottom row) showing tail, body, neck, head and uncinate parts of the pancreas. Note the homogeneous appearance of the pancreas on the stiffness maps. (Image courtesy- Dr. Yu Shi, Radiology, Shengjing hospital, China Medical University, Shenyang, Liaoning, China)

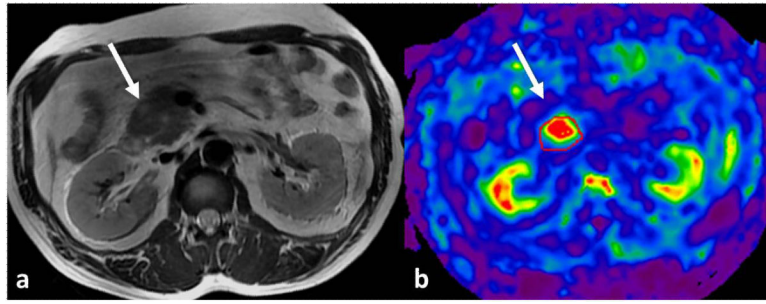


Fig.11. MRE of pancreas performed at 40Hz. Axial T2-weighted image (a) shows a mildly hyperintense mass in the head of pancreas representing histology proven well differentiated adenocarcinoma. Stiffness map (b) showing increased stiffness of the mass at 2.9kPa, significantly higher than normal pancreas stiffness of 1.1kPa (Image courtesy- Dr. Yu Shi, Radiology, Shengjing hospital, China Medical University, Shenyang, Liaoning, China).

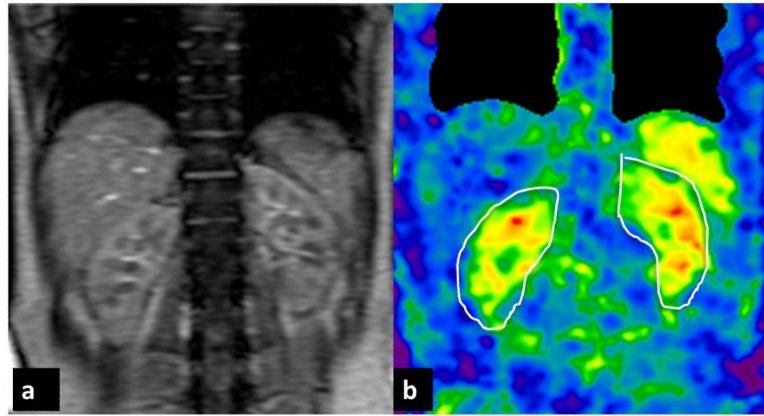


Fig. 12. MRE of the native kidneys performed at 90Hz in coronal plane in a normal healthy volunteer. A single large driver was placed in midline with the volunteer lying supine over the driver. Stiffness map (b) demonstrating symmetrical stiffness distribution in the kidneys (outlined). The mean stiffness of the kidneys was 6.4kPa.

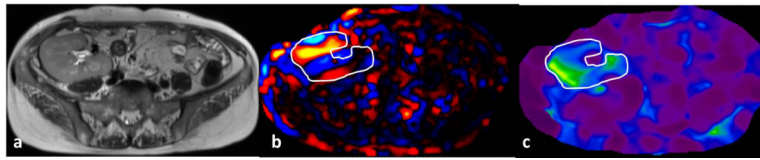


Fig.13.

MRE of a normal functioning transplant kidney performed at 90Hz. Axial T2-weighted image (a) showing a normal size renal graft in the right iliac fossa. Wave image (b) demonstrating propagation of shear waves through the graft and a stiffness map (b) with graft outlined. The mean stiffness of the graft was 6.8kPa.

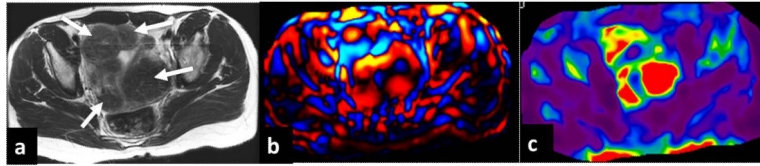


Fig.14.

MRE of a fibroid uterus performed at 60Hz. Axial T2-weighted image (a) showing several hypointense fibroids (arrows), wave image (b) showing excellent propagation of the shear waves through the uterus and fibroids. Stiffness map (c) showing stiff areas corresponding to the fibroids.